

Synthesis of Xenon and Iron-Nickel Intermetallic Compounds at Earth's Core Thermodynamic Conditions

Elissaios Stavrou,^{1,*} Yansun Yao,^{2,3,†} Alexander F. Goncharov,^{4,5,6,‡} Sergey S. Lobanov,^{5,7}

Joseph M. Zaug,¹ Hanyu Liu,⁵ Eran Greenberg,⁸ and Vitali B. Prakapenka⁸

¹Lawrence Livermore National Laboratory, Physical and Life Sciences Directorate, Livermore, California 94550, USA

²Department of Physics and Engineering Physics, University of Saskatchewan, Saskatoon Saskatchewan S7N 5E2, Canada

³Canadian Light Source, Saskatoon, Saskatchewan S7N 2V3, Canada

⁴Key Laboratory of Materials Physics and Center for Energy Matter in Extreme Environments, Chinese Academy of Sciences, Hefei 230031, China

⁵Geophysical Laboratory, Carnegie Institution of Washington, Washington, D.C. 20015, USA

⁶University of Science and Technology of China, Hefei 230026, China

⁷Sobolev Institute of Geology and Mineralogy, Siberian Branch Russian Academy of Science, Novosibirsk 630090, Russia

⁸Center for Advanced Radiation Sources, University of Chicago, Chicago, Illinois 60637, USA



(Received 25 July 2017; published 28 February 2018)

Using *in situ* synchrotron x-ray diffraction and Raman spectroscopy in concert with first principles calculations we demonstrate the synthesis of stable $\text{Xe}(\text{Fe}, \text{Fe}/\text{Ni})_3$ and XeNi_3 compounds at thermodynamic conditions representative of Earth's core. Surprisingly, in the case of both the Xe-Fe and Xe-Ni systems Fe and Ni become highly electronegative and can act as oxidants. The results indicate the changing chemical properties of elements under extreme conditions by documenting that electropositive at ambient pressure elements could gain electrons and form anions.

DOI: [10.1103/PhysRevLett.120.096001](https://doi.org/10.1103/PhysRevLett.120.096001)

Noble gas elements (NGEs) are considered as the most chemically inert elements due to the closed subshell configuration that prevents the formation of stable compounds. However, recent theoretical studies [1–4] suggest that stable compounds between NGEs and metals (electropositive at ambient conditions elements) could be formed under high pressure conditions due to the substantial effect of pressure on the chemical properties. The stability of such compounds can be attributed to the changes of chemical properties of elements under pressure [1,5–7]. This includes altered electronegativity and reactivity, charge transfer between orbitals and/or constitution elements, and the appearance of multicenter bonding and electronegative states [8]. In general, for the predicted stable compounds of NGEs and metals either a NGE can gain electrons from an electropositive, at the corresponding pressures, element [3], or a metal becomes electronegative and acts as an oxidant (e.g., the Xe-Fe/Ni system [1]). The latter case is unusual and counters chemical intuition because it implies that Fe and Ni become more electronegative than Xe. Experimental realization of such compounds is incomplete highlighting the necessity of experimental verification of theory to better understand the chemistry at extreme conditions and, thus, advance the chemistry and physics of highly compressed material states.

The formation of stable Xe-Fe(Ni) compounds would also change our understanding about the presence of Xe in

Earth's core. According to the simple mass fractionation model (see the discussion in Refs. [9,10] and references therein), heavy NGEs should be less depleted and isotopically fractionated in comparison to the lighter ones, in agreement with observations in meteorites. However, in Earth's atmosphere, Xe is more depleted than Kr and more fractionated than both Kr and Ar [9]. These two observations constitute one of the most challenging open questions in the geosciences [9,11], and give rise to the so-called “missing Xe paradox.” Although various models have been suggested on the origin of the Xe depletion [12], it is commonly attributed to the inclusion of Xe in Earth's interior [10]. While Xe was reported to form compounds with water ice [13] and quartz [14], none of them provide a plausible explanation to the missing Xe paradox [15]. The successful formation of xenon oxides under deep mantle conditions has been recently reported [16]. However, the presence of such compounds is precluded by the lack of free oxygen in Earth's mantle.

Accordingly, a hypothesis of stable Xe-Fe/Ni compounds in Earth's core was proposed as an explanation for the “missing” Xe [10]. In this scenario, other NGEs are not missing due to the much more extreme thermodynamic conditions needed for the formation of stable compounds [3]. Previous experimental attempts did not trace the formation of Fe-Xe compounds up to 200 GPa and below 2500 K [17–19] and this has been attributed to the large size difference between Xe and Fe ions, which hinders the

formation of Xe-Fe solid solutions according to the Hume-Rothery rule [18]. A recent theoretical study [1], using *ab initio* calculations combined with structural search methods, suggests that Xe-Ni and Xe-Fe compounds are thermodynamically stable above 150 GPa and 200 GPa, respectively. The stability of these compounds is enhanced at elevated temperatures (>2000 K), i.e., at thermodynamic conditions representative of Earth's outer core. The predicted crystal structures of Xe-Fe/Ni compounds are distinct from the structures of elemental Xe, Fe, and Ni at the same thermodynamic conditions. This suggests that the formation mechanism of these compounds goes beyond a simple element substitution.

In this study, we explored the possible formation of stable compounds in the Xe-Fe/Ni system at thermodynamic conditions representative of Earth's core by performing high pressure experiments in a laser-heated diamond-anvil cell starting from the following mixtures: (a) Xe-Fe, (b) Xe-Fe/Ni alloy ($\sim 7\%$ Ni), and (c) Xe-Ni. Using *in situ* synchrotron x-ray diffraction and Raman spectroscopy we successfully identified the formation of (a) a $\text{XeFe}_3/\text{Xe}(\text{Fe}_{0.93}\text{Ni}_{0.07})_3$ compound, characterized as a mixture of a fcc and an orthorhombic NbPd_3 -type structure, above 200 GPa and 2000 K, and (b) a XeNi_3 compound, in the form of a CrNi_3 -type fcc structure, above 150 GPa and 1500 K. Preliminary data on all these observations have been reported at the American Geophysical Union 2015 Fall meeting [20]. We find the formation of XeFe_3 compounds above 200 GPa (in contrast with previous studies [19]) while XeNi_3 forms at much lower pressure signifying the importance of the elemental electronic structure. The experimental results were examined and supported in synergy with a theoretical *ab initio* structural search and optimization. The formation of XeFe_3 and XeNi_3 compounds is kinetically driven with the structures identified in close proximity to the computed energy minima. The theoretical reaction threshold pressures for both compounds are in very good agreement with the experiment.

For the case of the Fe-Ni alloy with a Ni concentration (7%–8%) representative of Earth's core [21,22] an iron Sikhote-Alin meteorite was used as a proxy after chemical and homogeneity characterization using energy-dispersive x-ray spectroscopy (see Fig. S1 of the Supplemental Material [23]). The XRD patterns of the Fe-Ni alloy used in this study are representative of a hcp structure [see Fig. 1(a)] with a negligible cell volume difference (Fig. S2 [23]), at a given pressure, from that of pure Fe (also in a hcp structure) in agreement with previous studies [42]. We performed laser-heated experiments on both the Xe-Fe and $\text{Xe-Fe}_{0.93}\text{Ni}_{0.07}$ systems at various pressures from 150 to above 210 GPa. No new Bragg peaks, signaling the formation of new compounds, were observed below 195 GPa even after a prolonged laser heating above 3500 K, see Fig. S3 [23]. However, new Bragg peaks appeared for both mixtures after laser heating at ~ 2200 K and pressures >200 GPa,

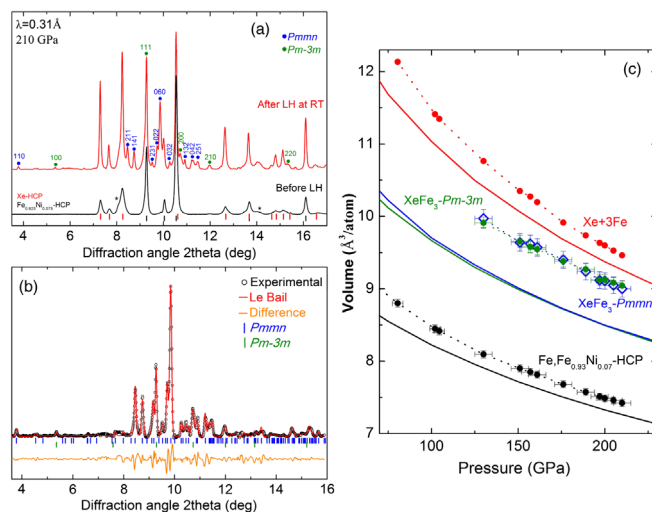


FIG. 1. (a) XRD patterns of the $\text{Xe-Fe}_{0.93}\text{Ni}_{0.07}$ mixture before and after laser heating at 210 GPa. New Bragg peaks after laser heating and the corresponding Miller indices for the $Pm-3m$ and the $Pmnm$ XeFe_3 crystal structures are noted with green and blue dots, respectively. The peak marked by the asterisk corresponds to the strongest peak of rhenium (gasket material). (b) Le Bail refinement of the $\text{Xe}(\text{Fe}_{0.93}\text{Ni}_{0.07})_3$ compound at 210 GPa. The peaks of the $Pm-3m$ and $Pmnm$ (1) structures are marked with green and blue vertical lines, respectively. (c) EOSs of Fe and $\text{XeFe}_3/\text{Xe}(\text{Fe}_{0.93}\text{Ni}_{0.07})_3$ as determined experimentally (dashed curves and solid symbols) and theoretically (solid curves) in this study. The volume of the superposition of $(\text{Xe} + 3\text{Fe})/4$ is also shown for comparison. The x-ray wavelength is 0.31 \AA .

implying an approximately 200 GPa reaction threshold, see Fig. 1(a) and Fig. S4(b) [23]. XRD patterns of the Xe-Fe and $\text{Xe-Fe}_{0.93}\text{Ni}_{0.07}$ systems after laser heating [Fig. S4(a) [23]] are essentially identical. Thus, we suggest that the presence of a low-concentration of Ni in the Fe-Ni alloy has no effect on the structure of the synthesized compound. Bragg peaks of pure Ni or a $\text{Fe}_{0.97}\text{Ni}_{0.07}$ bcc structure [21] were not observed during or after laser heating. Consequently, the possibility of phase separation or a phase transition is ruled out.

The new peaks in XRD patterns after the laser heating of the Xe-Fe and $\text{Xe-Fe}_{0.93}\text{Ni}_{0.07}$ mixtures cannot be indexed solely with the fcc ($Pm-3m$) XeFe_3 structure (Cu_3Au type) predicted by Zhu *et al.* [1] due to a much higher number of observed Bragg peaks and the presence of low angle peaks [see Fig. 1(a)]. Moreover, no Raman active modes are expected for the Cu_3Au -type structure in contrast with our Raman spectroscopy measurements [Fig. S5(a) [23]]. We identified the products as a mixture of a fcc and an orthorhombic [namely, $Pmnm$ (1)] phase with competitive enthalpies as revealed in our theoretical calculations, Fig. 2(a). Details on the procedure we followed for the identification of the $Pmnm$ (1) phase can be found in the Supplemental Material [23] together with the relevant structural parameters including Wyckoff positions, see Table S1 [23]. The $Pmnm$ (1) and the fcc structures are closely related as both are close

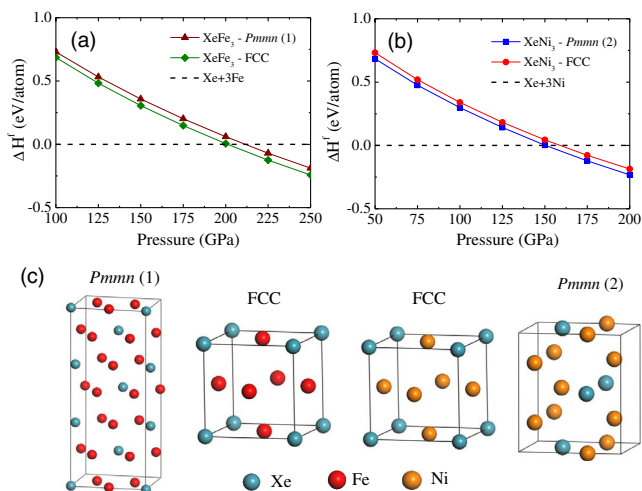


FIG. 2. Calculated enthalpies of formation ΔH^f of (a) XeFe_3 and (b) XeNi_3 with respect to the mixture of elemental Xe + 3Ni and Xe + 3Fe, respectively. The enthalpies of the fcc structure in both compounds were calculated in an ordered structure. The two $Pm\bar{m}n$ structures in XeFe_3 and XeNi_3 are distinctly different and therefore distinguished as $Pm\bar{m}n$ (1) and $Pm\bar{m}n$ (2). (c) Schematic representations of the corresponding structures of XeFe_3 and XeNi_3 .

packed with 12-fold coordinated Fe and Xe atoms. As a result, the volumes of these two structures are essentially degenerate above 100 GPa [Fig. 1(c)].

The Bragg peaks of the experimental XRD patterns can be very well indexed with a mixture of $Pm\bar{m}n$ (1) and $Pm\bar{3}m$ structures. However, preferred orientation and strongly anisotropic peak broadening effects, usual in High-pressure and High-temperature synthesis [43], prevent us from a full structural refinement (Rietveld) of the positional parameters due to differences between the observed and calculated intensities. A difference in the relative intensities could also arise from a positional disordered phase. For this reason, we have considered a positionally disordered $Pm\bar{m}n$ (1) structure with a Xe (25%)-Fe (75%) site occupancy. This structure has a negligible enthalpy difference from the ordered $Pm\bar{m}n$ (1) one and provides a better agreement with the experimental XRD patterns at the low 2θ (high- d) range, i.e., the range that is mainly affected by a difference between an ordered and a positionally disordered structure. In Fig. 1(b) we show the Le Bail refinement of the experimentally observed diffraction pattern based on a mixture of $Pm\bar{m}n$ (1) [with Xe(25%)-Fe (75%)] and $Pm\bar{3}m$ structures, after subtracting [see Ref. [44] and Fig. S3(c) [23] for a representative example] the Fe and Xe related Bragg peaks.

Raman experiments on samples quenched to 300 K [Fig. S5(a) [23]] show the presence of a new broad weak peak at $450 - 480 \text{ cm}^{-1}$. Low intensity Raman spectra are consistent with the formation of a metallic or semimetallic XeFe_3 compound [1] and consequently only the highest

intensity peaks are expected to be observed. The position of the observed Raman peak is indeed in agreement with the strongest calculated peak of the $Pm\bar{m}n$ (1) XeFe_3 phase. The fcc XeFe_3 compound is not expected to have any Raman activity. Thus, the presence of the Raman bands strongly supports the existence of a second $Pm\bar{m}n$ (1) phase in addition to fcc XeFe_3 . Moreover, the pressure slope of the experimentally observed peak and of the most intense peak of the calculated Raman spectrum [Fig. S5(b) [23]] agree well, thus, providing an additional argument in favor of the synthesis of the $Pm\bar{m}n$ (1) XeFe_3 phase.

The experimentally determined volume of XeFe_3 is 5% lower than that of the 1:3 solid mixture of Xe and Fe and the theoretical EOS yields the same trend, with the XeFe_3 having an 8% smaller volume than the mixture, see Fig. 1(c). Compared to the experimental values, the theoretical volumes of Fe and $\text{XeFe}_3/\text{Xe}(\text{Fe}_{0.93}\text{Ni}_{0.07})_3$ are clearly underestimated. Here, a possible source of error is the well-known insufficiency of standard density functional theory treating the ground state of Fe, which was shown to be largely affected by dynamical many-body effects [45]. Nevertheless, experiment and theory agree in that XeFe_3 has a smaller volume than its constituents, suggesting, together with the lower enthalpy, that this compound is thermodynamically favored. On pressure release, both the XeFe_3 and the $\text{Xe}(\text{Fe}_{0.93}\text{Ni}_{0.07})_3$ compounds remain stable down to, at least, 127 GPa (Fig. S6 [23]) followed by a decomposition to Xe and Fe/ $\text{Fe}_{0.93}\text{Ni}_{0.07}$ at lower pressures.

Figure 3(a) shows XRD patterns of the Xe-Ni mixture at 155 GPa before laser heating, upon increasing the temperature and at RT after laser heating. The XRD pattern before laser heating is representative of a heterogeneous mixture of hcp-Xe [46] and fcc-Ni. With increasing temperature the Ni Bragg peaks completely disappear above 1500 K while new peaks appear concomitantly suggesting that Ni fully reacts towards the formation of a new compound that remains stable after quenching to RT. Xe related Bragg peaks remain present suggesting conditions of Xe excess in the cavity. The new Bragg peaks can be indexed with an A1 fcc unit cell with a cell volume representative of a XeNi_3 compound. This attribution is based on the comparison between the atomic volumes of the synthesized compound, Ni, and Xe at the same pressure [see Figs. S7 and S8(b) [23]]. Fulfillment of the extinction conditions of A1 by the observed reflections implies the formation of a CrNi_3 -type binary alloy with Xe and Ni distributed randomly or statistically over the fcc sites. An ordered fcc structure (Cu_3Au type) would have several additional low intensity Bragg peaks [see Fig. 3(b)], which are absent in the XRD pattern of XeNi_3 .

The synthesized XeNi_3 compound remains stable up to at least 100 GPa upon pressure release, see Fig. S8(a) [23]. Significantly, both the experimentally determined and calculated volumes of XeNi_3 are 10% smaller than that of the 1:3 solid mixture of Xe and Ni, suggesting that the

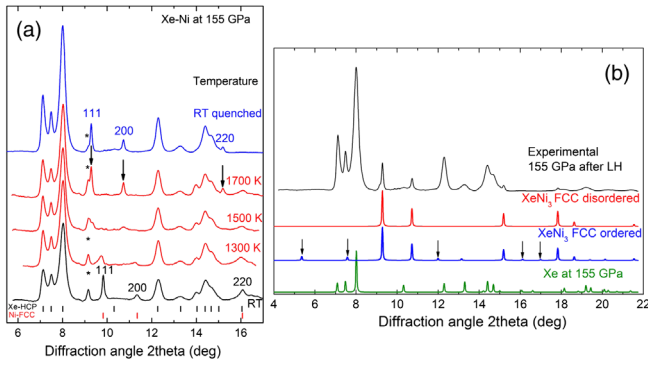


FIG. 3. (a) XRD patterns of a Xe-Ni mixture at 155 GPa as a function of temperature. The peak marked by the asterisk corresponds to the strongest peak of rhenium. The peaks of the hcp-Xe and fcc-Ni at RT before laser heating are marked with black and red vertical ticks, respectively. The vertical arrows mark the position of the Bragg peaks of the XeNi₃ compound. The corresponding Miller indices for the fcc-Ni and the fcc-XeNi₃ are noted before and after laser heating, respectively. (b) XRD pattern of the synthesized XeNi₃ compound in comparison to the calculated patterns of ordered (blue) and disordered (red) fcc crystal structures. The calculated pattern of the hcp-Xe is also shown for comparison. The vertical arrows mark the position of the additional Bragg peaks expected in an ordered Cu₃Fe-type fcc structure. The x-ray wavelength is 0.310 Å.

former is a stable compound [Fig. S7(b) [23]]. However, exact stoichiometry of the synthesized compound may not be precisely determined. Nevertheless, both the experimentally determined equation of state (EOS) and the predicted stability of the XeNi₃ compound strongly suggest a composition very close, if not exact, to XeNi₃. The thermodynamic stability of the XeNi₃ compound was investigated through the relative enthalpy of formation, ΔH^f , with respect to a 1:3 solid mixture of Xe and Ni [Fig. 2(b)]. The fcc structure is comparable in enthalpy with the *Pmnm* structure [named here as *Pmnm* (2)] predicted by Zhu *et al.* [1]. The ΔH^f of the fcc structure is slightly higher than the latter one, i.e., by ~ 0.04 eV/atom, indicating a metastable structure close to the global minimum.

Considering that the formation of XeNi₃ only takes place at high temperature it is reasonable to suggest that the synthesis of this compound is kinetically driven [47,48]. The ΔH^f of the fcc structure approaches zero near 158 GPa, which corresponds very well with the experimental reaction threshold of 155 GPa. Both fcc and *Pmnm* (2) structures are close packed with 12-fold coordinated Ni and Xe atoms [Fig. 2(c)], which explains their similar enthalpies. The enthalpy change due to the positional disorders of Xe and Ni was estimated using a fcc supercell of 256 atoms. A set of 200 structures was generated by placing Xe and Ni atoms randomly at the fcc lattice sites, each representing a possible solid solution configuration. The calculated enthalpies of these structures (at 150 GPa) are within a 0.1 eV/atom range above the enthalpy of the ordered fcc structure.

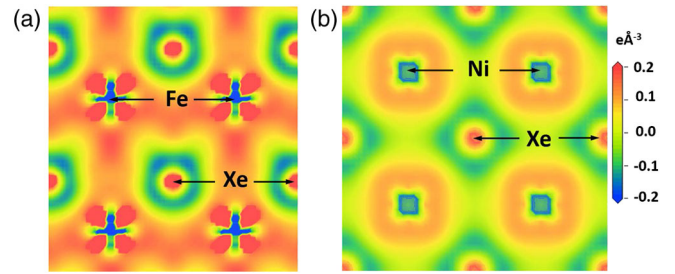


FIG. 4. Calculated deformation charge density of XeFe₃ in the (010) plane (a) and XeNi₃ in the (001) plane (b) at 200 GPa.

Recently, Dewaele *et al.* [19] reported the synthesis of a stable XeNi₃ compound with an ordered fcc structure. Although the reported stoichiometry, the reaction threshold, the volume per atom and the fundamental crystal structure are in agreement with this work (see also Ref. [20]) a discrepancy exists on the detailed crystal structure, i.e., ordered versus disordered fcc. This can be attributed to differences in the quenching time. The formation of an ordered structure requires substantial atomic diffusion, which is likely restricted by the fast kinetics in the present case, i.e., the quenching process. Strictly speaking, in a positional disordered structure the volume is a statistical average, which may deviate slightly from that of an ordered structure. The present calculation reveals that the deviation is negligible in the present thermodynamic scale, which is further justified by the agreement of the reported experimental volumes per atom (Fig. S7 [23]).

The successful synthesis of Xe-Ni/Fe compounds in this study, well supported and corroborated by the theoretical calculations of the present study and a previous study by Zhu *et al.* [1], can be attributed to the changing chemical properties of elements under pressure. This trend is clearly demonstrated by the calculated deformation charge density of XeFe₃ and XeNi₃, defined as the difference between the charge density of the crystal and the superimposed charge densities of noninteracting atoms [Figs. 4(a) and 4(b)]. In both cases, electrons are removed from Xe (positive regions, red) and transferred to the metals (negative regions, blue). According to previous theoretical studies (e.g., Refs. [1,7]), the application of pressure dramatically affects the chemical properties of elements. Fe and Ni, in particular, become highly electronegative and can act as oxidants in compounds. Xe, on the other hand, opens up the fully filled 5*p* states as valence states. The charge transfer therefore takes place between the Xe 5*p* states and the partially filled Fe/Ni 3*d* or 4*s* (if an *s* to *d* transition occurs in Fe/Ni) states. Mulliken's analysis of electron density reveals the amounts of transferred charge in XeFe₃ and XeNi₃ are $0.64e/\text{Xe}$ and $0.52e/\text{Xe}$, respectively, at 200 GPa. A greater amount of charge transfer in XeFe₃, which is visible in Fig. 4(a), is consistent with a lower occupation (*d*⁶) in the 3*d* states of Fe as compared to the *d*⁸ occupation of Ni. The different amounts of charge transfer

also likely affect the reaction pressures for these two compounds.

Our experiments document that stable compounds of metals and NGEs can exist under pressure, stabilized by a major electron transfer from Xe to Fe and Ni. For comparison, much lower electron transfers between Na-He ($-0.174e/\text{He}$) and Cs-Xe (-0.14 to $-0.18e/\text{Xe}$) were calculated in the cases of the synthesized Na_2He [8] and predicted CsXe_2 [4] compounds, respectively. This highlights a bonding scheme that is quite different from the ones in the cases of (a) Van der Waals Xe- H_2 and Xe- N_2 compounds stabilized at elevated pressures [49,50], and (b) compounds between alkali and alkali earth metals and NGEs. This bonding pattern resembles more the bonding between high-Z NGEs, such as Xe and Kr, and strong electronegative elements such as F [51,52] and Cl and O [53] at ambient pressure. Thus, our study signifies a near halogenlike behavior of Fe and Ni under high-pressure conditions in agreement with theoretical predictions [1,7].

The possible formation of stable Xe-Fe compounds at Earth's core thermodynamic conditions was previously considered [1,10,18] as a possible explanation of Xe depletion in Earth's atmosphere. Although our study provides the first experimental evidence of the stability of Xe-Fe compounds at relevant thermodynamic conditions, it is unlikely that such compounds have been formed during Earth's core accretion. The formation pressure of such compounds (200 GPa), as determined in this work, is too high compared to that suggested for Earth's core accretion pressure (near 50 GPa) using geochemical arguments [54]. Moreover, Mars' atmosphere is also depleted in Xe while the martian core pressure is ~ 40 GPa while it is plausible to assume that Xe depletion likely stems from the same process for both planets. This suggests that the formation of XeFe_3 is an unlikely explanation of the missing Xe paradox and thus, alternative, to Earth's core reservoir, scenarios should be considered [17]. Alternatively, a two step mechanism should be considered: an increased solubility of Xe in molten Fe at lower accretion pressures followed by a reaction at higher pressures. However, this extends beyond the scope of this work and calls for follow-up relevant studies.

The authors thank Zurong Dai for assistance with the SEM/EDX measurements and Sergey N. Tkachev for helping with the gas loading at sector 13 GSECARS. Part of this work was performed under the auspices of the U.S. DOE by LLNS, LLC under Contract No. DE-AC52-07NA27344. This work was supported by the DARPA (Grant No. W31P4Q1210008), the Deep Carbon Observatory, the Army Research Office, and the Natural Sciences and Engineering Research Council of Canada. A. F. G. was partly supported by a Chinese Academy of Sciences visiting professorship for senior international scientists (Grant No. 2011T2J20) and the Recruitment Program of Foreign Experts) and the National Natural

Science Foundation of China (Grants No. 21473211 and No. 11674330). S. S. L. was partly supported by the state assignment project (No. 0330-2016-0006). H. L. was supported by the Energy Frontier Research Center funded by the DOE, Office of Science, BES (Award No. DE-SC-0001057). GSECARS is supported by the U.S. NSF (Grant No. EAR-1128799) and DOE Geosciences (Grant No. DE-FG02-94ER14466). The ALS is supported by the Director, Office of Science, BES of DOE under Contracts No. DE-AC02-05CH11231 and No. DE-AC02-06CH11357. Computing resources were provided by the University of Saskatchewan, Westgrid, and Compute Canada. We thank Cheng Ji, Dave Mao, and Rich Ferry for enabling the Raman measurements at HPSynC, APS. This work was partially funded by a Laboratory Directed Research and Development Program project (18-LW-036).

The authors declare no competing financial interests.

*stavroul@llnl.gov

†yansun.yao@usask.ca

‡alex@issp.ac.cn

- [1] L. Zhu, H. Liu, C. J. Pickard, G. Zou, and Y. Ma, *Nat. Chem.* **6**, 644 (2014).
- [2] X. Li, A. Hermann, F. Peng, J. Lv, Y. Wang, H. Wang, and Y. Ma, *Sci. Rep.* **5**, 16675 (2015).
- [3] M.-S. Miao, X.-l. Wang, J. Brgoch, F. Spera, M. G. Jackson, G. Kresse, and H.-q. Lin, *J. Am. Chem. Soc.* **137**, 14122 (2015).
- [4] S. Zhang, H. Bi, S. Wei, J. Wang, Q. Li, and Y. Ma, *J. Phys. Chem. C* **119**, 24996 (2015).
- [5] W. Grochala, R. Hoffmann, J. Feng, and N. W. Ashcroft, *Angew. Chem., Int. Ed. Engl.* **46**, 3620 (2007).
- [6] Q. Zhu, D. Y. Jung, A. R. Oganov, C. W. Glass, C. Gatti, and A. O. Lyakhov, *Nat. Chem.* **5**, 61 (2013).
- [7] G. Q. X. Dong, A. R. Oganov, Q. Z. X-F. Zhou, and H.-T. Wang, *arXiv:1503.00230*.
- [8] X. Dong, A. R. Oganov, A. F. Goncharov, E. Stavrou, S. Lobanov, G. Saleh, G.-R. Qian, Q. Zhu, C. Gatti, V. L. Deringer, R. Dronskowski, X.-F. Zhou, V. B. Prakapenka, Z. Konôpková, I. A. Popov, A. I. Boldyrev, and H.-T. Wang, *Nat. Chem.* **9**, 440 (2017).
- [9] N. Dauphas, *Icarus* **165**, 326 (2003).
- [10] K. K. M. Lee and G. Steinle-Neumann, *J. Geophys. Res.* **111**, B02202 (2006).
- [11] E. Anders and T. Owen, *Science* **198**, 453 (1977).
- [12] S. S. Shcheka and H. Keppler, *Nature (London)* **490**, 531 (2012).
- [13] C. Sanloup, S. A. Bonev, M. Hochlaf, and H. E. Maynard-Casely, *Phys. Rev. Lett.* **110**, 265501 (2013).
- [14] C. Sanloup, B. C. Schmidt, E. M. C. Perez, A. Jambon, E. Gregoryanz, and M. Mezouar, *Science* **310**, 1174 (2005).
- [15] M. I. J. Probert, *J. Phys. Condens. Matter* **22**, 025501 (2010).
- [16] A. Dewaele, N. Worth, C. J. Pickard, R. J. Needs, S. Pascarelli, O. Mathon, M. Mezouar, and T. Irifune, *Nat. Chem.* **8**, 784 (2016).

- [17] W. A. Caldwell, J. H. Nguyen, B. G. Pfrommer, F. Mauri, S. G. Louie, and R. Jeanloz, *Science* **277**, 930 (1997).
- [18] D. Nishio-Hamane, T. Yagi, N. Sata, T. Fujita, and T. Okada, *Geophys. Res. Lett.* **37**, L04302 (2010).
- [19] A. Dewaele, C. M. Pépin, G. Geneste, and G. Garbarino, *High Press. Res.* **37**, 137 (2017).
- [20] E. Stavrou, M. J. Zaug, J. Crowhurst, S. Lobanov, A. F. Goncharov, V. Prakapenka, C. Presche, Y. Yao, H. Liu, and Z. Dai, in *American Geophysical Union Fall Meeting, San Francisco* (2015), <https://agu.confex.com/agu/fm15/meetingapp.cgi/Search/0?>.
- [21] L. Dubrovinsky, N. Dubrovinskaia, O. Narygina, I. Kantor, A. Kuznetsov, V. B. Prakapenka, L. Vitos, B. Johansson, A. S. Mikhaylushkin, S. I. Simak, and I. A. Abrikosov, *Science* **316**, 1880 (2007).
- [22] W. F. Bottke, D. Nesvorný, R. E. Grimm, A. Morbidelli, and D. P. O'Brien, *Nature (London)* **439**, 821 (2006).
- [23] See Supplemental Material at <http://link.aps.org/supplemental/10.1103/PhysRevLett.120.096001>, which includes Refs. [24–41], for methods, the procedure followed for the identification of the *Pmmn* (1) phase, and supplemental Figs. S1–S8.
- [24] C. Prescher and V. B. Prakapenka, *High Press. Res.* **35**, 223 (2015).
- [25] W. Kraus and G. Nolze, *J. Appl. Crystallogr.* **29**, 301 (1996).
- [26] A. C. Larson and R. B. V. Dreele, Technical Report No. LAUR 86-748, Los Alamos National Laboratory, 2000.
- [27] A. Boultif and D. Louër, *J. Appl. Crystallogr.* **37**, 724 (2004).
- [28] V. B. Prakapenka, A. Kubo, A. Kuznetsov, A. Laskin, O. Shkurikhin, P. Dera, M. L. Rivers, and S. R. Sutton, *High Press. Res.* **28**, 225 (2008).
- [29] M. Kunz, A. MacDowell, W. Caldwell, D. Cambie, R. Celestre, E. Domning, R. Duarte, A. Gleason, J. Glossinger, N. Kelez, D. Plate, T. Yu, J. Zaug, H. Padmore, R. Jeanloz, A. Alivisatos, and S. Clark, *J. Synchrotron Radiat.* **12**, 650 (2005).
- [30] E. Stavrou, M. Ahart, M. F. Mahmood, and A. F. Goncharov, *Sci. Rep.* **3**, 1290 (2013).
- [31] G. Kresse and J. Hafner, *Phys. Rev. B* **47**, 558 (1993).
- [32] G. Kresse and D. Joubert, *Phys. Rev. B* **59**, 1758 (1999).
- [33] J. P. Perdew, K. Burke, and M. Ernzerhof, *Phys. Rev. Lett.* **77**, 3865 (1996).
- [34] R. Martoňák, A. Laio, and M. Parrinello, *Phys. Rev. Lett.* **90**, 075503 (2003).
- [35] R. Martoňák, D. Donadio, A. R. Oganov, and M. Parrinello, *Nat. Mater.* **5**, 623 (2006).
- [36] A. Fonari and S. Stauffer, *vaspraman.py*, <https://github.com/raman-sc/VASP/>, 2013.
- [37] B. C. Giessen and N. J. Grant, *Acta Crystallogr.* **17**, 615 (1964).
- [38] P. Lazor, Ph.D. thesis, Uppsala University, 1994.
- [39] S. Merkel, A. F. Goncharov, H.-k. Mao, P. Gillet, and R. J. Hemley, *Science* **288**, 1626 (2000).
- [40] A. F. Goncharov, E. Gregoryanz, H. K. Mao, R. J. Hemley, N. Boctor, and E. Huang, *Raman Scattering of Metals to Very High Pressures, High-Pressure Phenomena, Proceedings of the International School of Physics, Enrico Fermi Course CXLVII*, edited by R. J. Hemley, M. Bernasconi, L. Ulivi, and G. Chiarotti (IOS Press, Amsterdam, 2002).
- [41] Y. A. Freiman, A. F. Goncharov, S. M. Tretyak, A. Grechnev, J. S. Tse, D. Errandonea, H.-k. Mao, and R. J. Hemley, *Phys. Rev. B* **78**, 014301 (2008).
- [42] H. K. Mao, Y. Wu, L. C. Chen, J. F. Shu, and A. P. Jephcoat, *J. Geophys. Res.* **95**, 21737 (1990).
- [43] E. Stavrou, S. Lobanov, H. Dong, A. R. Oganov, V. B. Prakapenka, Z. Konôpková, and A. F. Goncharov, *Chem. Mater.* **28**, 6925 (2016).
- [44] V. V. Struzhkin, D. Y. Kim, E. Stavrou, T. Muramatsu, H.-k. Mao, C. J. Pickard, R. J. Needs, V. B. Prakapenka, and A. F. Goncharov, *Nat. Commun.* **7**, 12267 (2016).
- [45] L. V. Pourovskii, J. Mravlje, M. Ferrero, O. Parcollet, and I. A. Abrikosov, *Phys. Rev. B* **90**, 155120 (2014).
- [46] A. P. Jephcoat, H.-k. Mao, L. W. Finger, D. E. Cox, R. J. Hemley, and C.-s. Zha, *Phys. Rev. Lett.* **59**, 2670 (1987).
- [47] V. Ozolins, C. Wolverton, and A. Zunger, *Phys. Rev. B* **57**, 6427 (1998).
- [48] Z. W. Lu, S.-H. Wei, A. Zunger, S. Frota-Pessoa, and L. G. Ferreira, *Phys. Rev. B* **44**, 512 (1991).
- [49] M. Somayazulu, P. Dera, A. F. Goncharov, S. A. Gramsch, P. Liermann, W. Yang, Z. Liu, H.-k. Mao, and R. J. Hemley, *Nat. Chem.* **2**, 50 (2010).
- [50] R. T. Howie, R. Turnbull, J. Binns, M. Frost, P. Dalladay-Simpson, and E. Gregoryanz, *Sci. Rep.* **6**, 34896 (2016).
- [51] H. H. Claassen, H. Selig, and J. G. Malm, *J. Am. Chem. Soc.* **84**, 3593 (1962).
- [52] P. A. Agron, A. A. Mason, H. A. Levy, G. M. Begun, C. G. Jones, and D. F. Smith, *Science* **139**, 842 (1963).
- [53] D. F. Smith, *J. Am. Chem. Soc.* **85**, 816 (1963).
- [54] J. Li and C. B. Agee, *Nature (London)* **381**, 686 (1996).